Off-centred immobile magnetic vortex under influence of spin-transfer torque

2011 J. Phys. D: Appl. Phys. 44 285001

(http://iopscience.iop.org/0022-3727/44/28/285001)

IOP PUBLISHING JOURNAL OF PHYSICS D: APPLIED PHYSICS

J. Phys. D: Appl. Phys. **44** (2011) 285001 (7pp) doi:10.1088/0022-3727/44/28/285001

Off-centred immobile magnetic vortex under influence of spin-transfer torque

Volodymyr P Kravchuk[1], Denis D Sheka[1,2], Franz G Mertens[3] and Yuri Gaididei[1]

[1] Institute for Theoretical Physics, 03143 Kiev, Ukraine
[2] Taras Shevchenko National University of Kiev, 01601 Kiev, Ukraine
[3] Physics Institute, University of Bayreuth, 95440 Bayreuth, Germany

E-mail: vkravchuk@bitp.kiev.ua

Received 30 December 2010, in final form 2 May 2011
Published 24 June 2011
Online at stacks.iop.org/JPhysD/44/285001

Abstract
Formation of the 'dip' structure which foregoes switching of magnetic vortex polarity is studied numerically in magnetic nanodisc. A new method based on influence of the spin-transfer torque is used. The method allows one to obtain the dip structure for *immobile* vortex which significantly improves studying accuracy in comparison with the case of moving vortex. Free out-of-plane vortices as well as in-plane vortices pinned on hole defects are considered. It is shown that the process of the dip formation is different for free and pinned vortices and direction of the dip does not directly depend on the vortex polarity.

(Some figures in this article are in colour only in the electronic version)

1. Introduction

The control of magnetic nonlinear structures using an electrical current is of special interest for applications in spintronics [1, 2]. The spin-transfer torque acts on nonhomogeneities in magnetization distributions, in particular, on magnetic vortices. Typical structures are CPP-heterostructures, where current flows perpendicular to the plane: metallic nanopillars, in which vortex oscillations have been studied both experimentally [3, 4] and theoretically [5–8], and magnetic tunnel junctions with large output power of spin transfer vortex nano-oscillators [9, 10]. Alternative systems are CIP-structures, where current flows in the plane of the interface [11, 12]. Recently Shibata *et al* [13] used CIP-structure to demonstrate the effect of the spin-transfer torque on the vortex state magnetic nanodisc. The spin current excites the spiral motion of the vortex which finally relaxes to some shifted position. Such a picture is a result of a Thiele–like vortex dynamics, where the vortex does not change the shape during its motion and it is valid for the relatively small vortex shifts.

It was shown both theoretically [8, 14, 15] and experimentally [16–18] that the vortex core magnetization (so-called vortex polarity) can be switched on a picosecond time scale. This discovery demonstrates the potential of realizing all-electrically controlled magnetic memory devices, changing the direction of the modern spintronics [19, 20]. The physical picture of the vortex switching is essentially the same in all systems where the switching was observed, including vortex excitations by different kinds of magnetic field and spin-polarize currents [15, 16, 21–28]. The switching process of a moving vortex includes two main stages. The vortex structure is excited at the first stage by a pumping (fields or currents), leading to the creation of an out-of-plane dip near the moving vortex. The appearance of a dip structure was computed by micromagnetic simulations [29] and confirmed experimentally [27, 28]. When the pumping is strong enough, the dip amplitude can reach the maximum possible value (second stage), leading to a vortex–antivortex pair generation from the dip structure. Dynamics of a three body problem is described analytically; [8, 30, 31] it is accompanied by the annihilation of the vortex–antivortex pair, which finally causes the switching of the vortex polarity.

In this paper we predict the dip formation near the vortex under the influence of the current. We consider two geometries, nanodisc and nanoring with small inner hole: symmetric as well as asymmetric (inner hole is shifted from disc centre). The spin current in the latter case provides the pure planar vortex centred

on inner hole of the ring. Using micromagnetic simulations[4] we discovered that such a shifted *immobile* vortex gets an extra out-of-plane magnetization which corresponds to the well-known 'dip' structure of the moving vortex [21, 23, 27]. Our study shows that the dip development is specified by the current direction and its intensity, and it does not depend on the vortex polarity. We also show that the critical current (threshold of the vortex–antivortex pair nucleation) strongly depends on the nanodot thickness for the ring geometry and this dependence is weak for disc geometry.

2. Model, micromagnetic simulations and a dip formation

Our study is based on a simulated magnetization dynamics in the framework of the modified Landau–Lifshitz–Gilbert (mLLG) equation with the CIP spin-torque effect [11, 12]:

$$\dot{\boldsymbol{m}} = -\gamma \boldsymbol{m} \times \boldsymbol{H}_{\text{eff}} + \alpha \boldsymbol{m} \times \dot{\boldsymbol{m}} - (\boldsymbol{u} \cdot \boldsymbol{\nabla})\boldsymbol{m} + \beta \boldsymbol{m} \times [(\boldsymbol{u} \cdot \boldsymbol{\nabla})\boldsymbol{m}]. \quad (1)$$

Here $\boldsymbol{m} = \boldsymbol{M}/M_{\text{S}} = (\sqrt{1-m_z^2}\cos\phi; \sqrt{1-m_z^2}\sin\phi; m_z)$ is a normalized magnetization vector with M_{S} being the saturation magnetization, the overdot indicates derivative with respect to time, $\gamma > 0$ is gyromagnetic ratio, $\boldsymbol{H}_{\text{eff}}$ is the effective micromagnetic field, α is the Gilbert damping constant. The last two terms in equation (1) describe, respectively, adiabatic and nonadiabatic spin-torque terms. The velocity parameter $\boldsymbol{u}$ is proportional to the current density: $\boldsymbol{u} = -\boldsymbol{j}P\mu_{\text{B}}/(|e|M_{\text{S}})$, where μ_{B} is the Bohr magneton, e is the electron charge and P is the current polarization rate. The current density $\boldsymbol{j}$ is supposed to be spatially uniform and constant. Dimensionless constant β describes the degree of the nonadiabaticity. The mLLG equations (1) can be derived from the Lagrangian with a density $\mathscr{L} = \mathscr{G} - \mathscr{E}$ and a Gilbert dissipative function density $\mathscr{F} = \alpha M_{\text{S}}/(2\gamma)(\dot{\boldsymbol{m}})^2$. Here the gyroscopic term $\mathscr{G} = \frac{M_{\text{S}}}{\gamma}(1-m_z)\dot{\phi}$, and the energy density $\mathscr{E} = 4\pi M_{\text{S}}^2(\mathscr{E}_{\text{ex}} + \mathscr{E}_{\text{ms}} + \mathscr{E}_{\text{ST}}^{a} + \mathscr{E}_{\text{ST}}^{na})$. Here $\mathscr{E}_{\text{ex}} = \ell^2(\boldsymbol{\nabla}\boldsymbol{m})^2$ is the exchange energy density with $\ell = \sqrt{A/(4\pi M_{\text{S}}^2)}$ being the exchange length, where A is the exchange constant. The magnetostatic energy density $\mathscr{E}_{\text{ms}} = (8\pi)^{-1}\int \text{d}^3\boldsymbol{r}'(\boldsymbol{m}(\boldsymbol{r})\cdot\nabla)(\boldsymbol{m}(\boldsymbol{r}')\cdot\nabla')|\boldsymbol{r}-\boldsymbol{r}'|^{-1}$ in case of a thin sample can be reduced to the effective easy plane anisotropy: $\mathscr{E}_{\text{ms}} \approx m_z^2/2$ [32]. The energy density of adiabatic spin torque term has a form $\mathscr{E}_{\text{ST}}^{a} = (1-m_z)(\boldsymbol{u}\cdot\boldsymbol{\nabla}\phi)$, the contribution of nonadiabatic term $\mathscr{E}_{\text{ST}}^{na}$ we discuss later.

2.1. Dip formation on a free immobile vortex in a nanodisc

In order to describe the CIP spin-torque influence onto the vortex dynamics we discuss two different kinds of simulations. In the first one we consider the permalloy[5] disc with radius $L = 100\,\text{nm}$ and thickness $h = 20\,\text{nm}$. The ground state of such a disc is the out-of-plane vortex, situated at the disc origin, see figure 1, curve 1. Then the spin current velocity was switched on adiabatically: step-by-step we increased the value of velocity u by a small value. The sizes of the steps were sufficiently small to prevent the vortex polarity switching. On each step the full relaxation was achieved and the set of parameters was determined: position of the vortex centre s (in units of the disc radius L), position of the dip minimum s_{d} and also the dip depth m_{d}, see figure 1. When the current is not strong, the position of the vortex centre $\boldsymbol{s}(t)$ can be calculated from the Thiele approach [33, 34], where the vortex moves like a rigid particle, $\boldsymbol{m}(\boldsymbol{r}, t) = \boldsymbol{m}(\boldsymbol{r} - \boldsymbol{X}(t))$, here $\boldsymbol{X}$ denotes the vortex core position. The generalized Thiele equation under the action of CIP current can be written as follows [12]:

$$\boldsymbol{G} \times (\dot{\boldsymbol{X}} - \boldsymbol{u}) + \hat{D}(\alpha\dot{\boldsymbol{X}} - \beta\boldsymbol{u}) = \boldsymbol{F}_{\text{ms}}, \quad (2)$$

where $\boldsymbol{G} = 2\pi hpq\boldsymbol{e}_z$ is the gyrovector with $p = +1$ being vortex polarity and $q = +1$ being the vorticity; $\hat{D} \approx h\pi q^2 \ln(L/\ell)\hat{I}$ is the dissipation tensor with $\hat{I}$ being the identity matrix, and $\boldsymbol{F}_{\text{ms}}$ is the magnetostatic force. According to (2), the vortex, originally situated at the disc origin, starts to make a spiral motion and finally goes to some shifted position, which results from the balance between the spin-torque force $\boldsymbol{F}_{\text{ST}}^{a} = \boldsymbol{u} \times \boldsymbol{G}$ and the restoring magnetostatic force $\boldsymbol{F}_{\text{ms}} = -k\boldsymbol{s}$ [13]:

$$\boldsymbol{s} = \frac{1}{k}([\boldsymbol{G} \times \boldsymbol{u}] + \hat{D}\beta\boldsymbol{u}), \quad (3)$$

where k is magnetostatic spring constant [8]. When the nonadiabatic term is absent ($\beta = 0$) the vortex is shifted perpendicularly to the current direction, see inset (a) of figure 1. At that the vortex and dip displacements linearly depend on the applied current and only near the critical current, when the vortex–antivortex pair is nucleated, the dependence $s_{\text{d}}(u)$ is slightly influenced by nonlinear effects, see figure 2(a). Small rippling, which is observed on the dependence $s(u)$ for high currents, is a numerical effect and it is caused by weak pinning of the vortex core on the discretization mesh. When the nonadiabatic term is taken into account the vortex equilibrium trajectory is deflected from the described main direction by angle $\varepsilon \approx \arctan[\beta/2\ln(L/\ell)]$ along the direction of the vector $\boldsymbol{u}$, see inset (b) of the figure 1.

Let us discuss now the deviations from the rigid approach. When the current is absent the vortex is situated in the disc centre and the vortex core is surrounded by the ring-shaped

[4] We used the open source OOMMF code http://math.nist.gov/oommf/ with an extension package for spin-current simulations developed by IBM Zurich Research Laboratory http://www.zurich.ibm.com/st/magnetism/spintevolve.html.

[5] In all OOMMF simulation we used material parameters adopted for permalloy: the exchange constant $A = 1.3 \times 10^{-11}\,\text{J m}^{-1}$, the saturation magnetization $M_{\text{S}} = 8.6 \times 10^5\,\text{A m}^{-1}$, the anisotropy was neglected and damping was chosen close to natural value $\alpha = 0.01$ for simulations of magnetization dynamics and $\alpha = 0.1$ for simulations which result in a static relaxed state. The material parameters correspond to the exchange length $\ell \approx 5.3\,\text{nm}$. The mesh cell was chosen to be $3 \times 3 \times h\,\text{nm}$ for simulations with disc and $2 \times 2 \times h$ for simulations with the nanorings with h being the sample thickness.

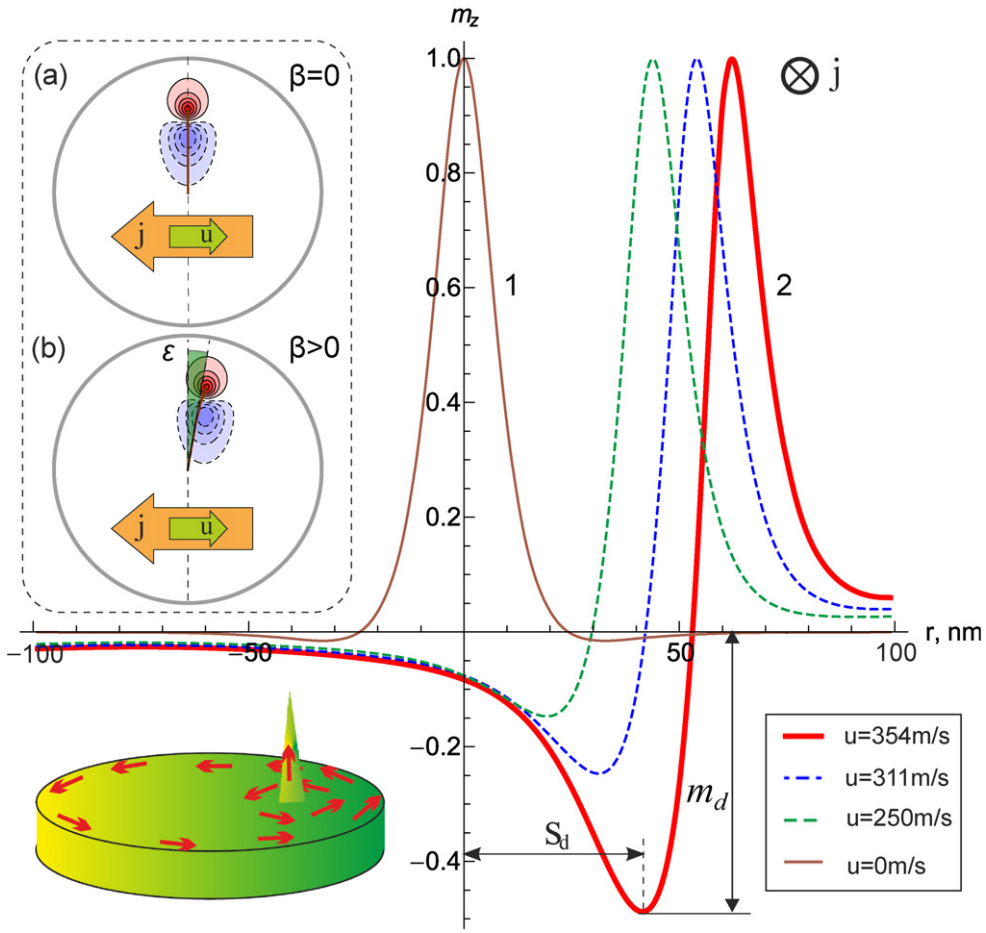

Figure 1. Profiles of the *immobile* equilibrium vortices for different values of the applied current. The profiles were taken along the diameter line perpendicular to the current direction (vertical dashed line on the insets) for case $\beta = 0$. The insets demonstrate the 2D distribution of the out-of-plane magnetization for current close to critical one: $\beta = 0$—inset (*a*) (the corresponding profile is shown with curve 2), and $\beta = 0.1$—inset (*b*). Dashed isolines correspond to the case $m_z < 0$ and solid isolines—to $m_z > 0$. Trajectory of the vortex core motion under *adiabatically slow* increasing of the current is shown as thick solid line in the insets. All presented data were obtained from the micromagnetic simulations of the permalloy nanodisc with radius $L = 100$ nm and thickness $h = 20$ nm.

area where $m_z < 0$, the so-called halo, see figure 1, curve 1. One should note that the halo effect is absent for the vortex in infinitesimally thin disc, where the nonlocal magnetostatic interaction is reduced to the local easy-plane anisotropy [8]. Such a halo has a magnetostatic nature: it appears due to the nonlocality of the magnetostatic interaction, namely as a result of interaction between face surface magnetostatic charges, produced by the vortex profile [8]. The halo amplitude is represented by the value $m_d(u = 0)$, see figure 2(*b*). When the current is switched on the vortex shifts and the halo becomes asymmetrical. As the current is increased the deepest part of the halo transforms to the dip structure, the dip amplitude increases and dependence $m_d(u)$ becomes essentially nonlinear, see figure 2(*b*). The nonadiabatic term does not influence the dependence $m_d(u)$ appreciably. Even for large nonadiabaticity with $\beta = 0.1$ [12] the maximum deviation $\max_u |\Delta m_d(u)| < 2 \times 10^{-3}$ and relative deviation of the critical current are also small: $\Delta j_c/j_c \approx 10^{-3}$. So the dependence $m_d(u)$ for case $\beta > 0$ is not shown in figure 2(*b*) because it practically coincides with the corresponding dependence for case $\beta = 0$.

The numerically obtained dependence $m_d(u)$ can be approximately fitted as follows:

$$m_d \propto \begin{cases} u & \text{when } u \ll u_c, \\ \sqrt{1 - \dfrac{u^2}{u_c^2}} - 1 & \text{when } u \lesssim u_c. \end{cases} \quad (4)$$

When the velocity u achieves some critical value u_c the dip structure becomes unstable and depth abruptly achieves its minimum value $m_d = -1$, hence the vortex–antivortex pair is born. Then the vortex polarity switching occurs accordingly with the well-studied scenario [21, 23]. It should be noted that the obtained critical velocity $u_c = 355\ \mathrm{m\,s^{-1}}$ is very close to the critical velocity for moving vortex [35]. To compare the dip structure of the moving vortex and dip structure of the immobile vortex under the spin-torque influence the following numerical experiment was performed: as an initial state the static vortex shifted by the current $j \lesssim j_c$ was chosen, then the current was switched off and the vortex motion to the disc centre by spiral trajectory was observed. At that the dependence $m_d(v)$ was calculated, were v is the velocity of

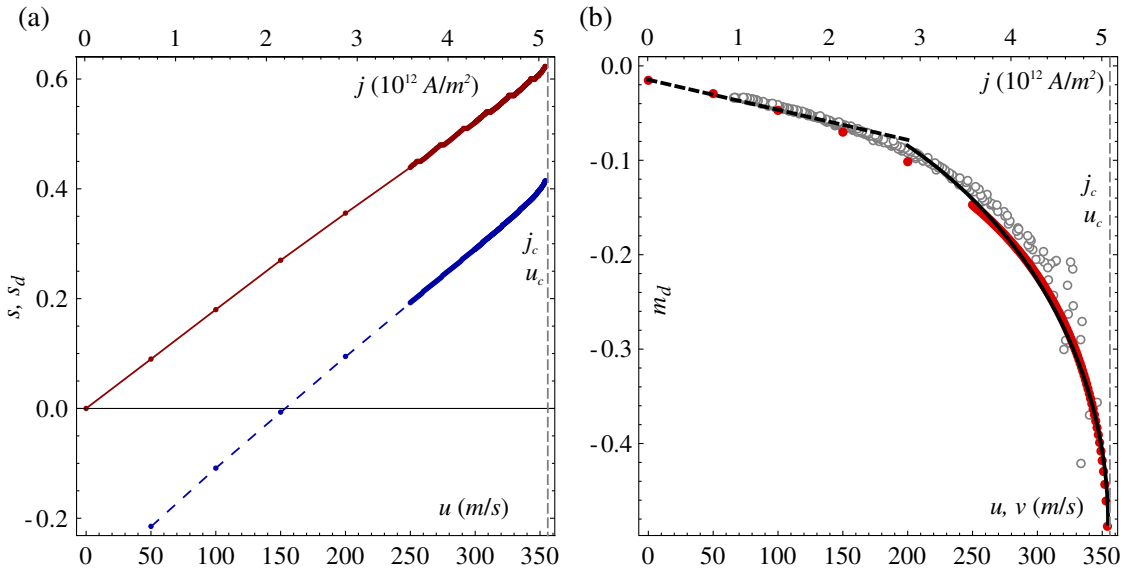

Figure 2. Parameters of the equilibrium vortex state depending on the applied current ($\beta = 0$). (*a*) shows the vortex (solid line) and dip (dashed line) displacement from the disc centre depending on the velocity u. The displacements are measured in units of L. (*b*) shows dependence of the dip depth m_d on u: points represent the simulation data and the curve corresponds to equation (4). The open circles correspond to the dip amplitude of the vortex during its free gyromotion without current versus velocity of the vortex core v. The vertical dashed line denotes the critical current u_c when the vortex–antivortex pair is born.

the vortex core. This dependence is shown in the figure 2(*b*) by open circles, where velocity v is measured along axis u. Since the obtained dependence $m_d(v)$ is very close to $m_d(u)$ one can conclude that the dip structure of the moving vortex is very similar to the dip structure of the immobile vortex under spin-torque influence and at that the current parameter u corresponds to the real velocity v.

To gain some insight into how the interaction with a current provides a dip creation, one should note that under the influence of strong enough current, the vortex displacement (3) becomes essential, hence the rigid approach is not valid. Instead, to describe in-plane vortex structure, the image-vortex ansatz [36] can be used:

$$\phi_v = \arg(\zeta - s) + \arg(\zeta - s_I) + \pi/2 - \arg s, \qquad (5)$$

where $\zeta = (x + iy)/L$ is a coordinate in the XY-plane, $s_I = s/s^2$ is the image vortex coordinate. In the linear approach on a small vortex shift s, in-plane magnetization structure can be described as $\phi_v(\rho, \chi) \approx \chi + s\rho \sin\chi$, where $\rho = |\zeta - s|$ and $\chi = \arg(\zeta - s)$ are the polar coordinates, measured from the centre of the shifted vortex centre (3). Qualitatively, the dip appears as a result of a balance between the magnetostatic energy term, $\mathscr{E}_{ms} = m_z^2/2$ and the spin-current one, $\mathscr{E}^a_{ST} = m_z(\boldsymbol{u}\cdot\boldsymbol{\nabla})\phi_v$. In such linear approach the dip corresponds to azimuthal magnon mode:

$$m_z \sim \frac{(\boldsymbol{u}\cdot\boldsymbol{\nabla})\,\phi_v}{2} \sim \frac{u\cos\chi}{2\rho}. \qquad (6)$$

Such estimation is valid only far from the vortex centre, and it corresponds to the asymptote $m_d \propto u$, see (4). In order to explain nonlinear behaviour, in particular, critical one, it is necessary to take into account nonlinear interaction between different magnon modes in the same way as we have done recently in [37, 38]. The theory of the dip creation will be published elsewhere.

2.2. Dip formation on a pinned immobile vortex in asymmetric nanoring

In order to study the role of the vortex out-of-plane structure in the dip formation process we performed the second kind of numerical experiment. With this end in view we considered the shifted vortex without out-of-plane component, the pure *immobile planar* vortex. The vortex was pinned on the small hole placed in the half of the disc radius. The hole radius r_h was chosen to be in the range $r_h \in (a_c; r_c \sim \ell)$, where a_c is the critical radius of the transition between out-of-plane and planar vortices [39], r_c is vortex core radius and ℓ is the exchange length (see footnote 5). Thus the hole radius r_h is big enough to make the vortex planar and it is small enough to prevent significant influence on the out-of-core magnetization structures. For thin permalloy films $a_c = 0.37\ell \approx 2$ nm [39] and $\ell \approx 5.3$ nm (see footnote 5). That is why we chose $r_h = 4$ nm. For simulation we chose the disc with $L = 100$ nm and $h = 10$ nm. The thickness decrease is needed for increasing the pinning effect due to decreasing the volume magnetostatic charges. In spite of the inner hole we suppose that the current j is spatially uniform in the simulations. Physically this can be achieved when the hole is filled by a nonmagnetic conductor with the conductivity close to the conductivity of the magnetic nanoring. In other words, the hole is considered in terms of the magnetization but not conductivity.

Let us consider the planar vortex which is pinned at the inner hole of the ring. In the case of the symmetric hole, the planar vortex forms a ground state of the disc, see figure 3(*b*). In the case of the asymmetric hole, the planar vortex is in an equilibrium state, which corresponds to the local energy minimum in the current absence. One can see from the figure 3 that the vortex does not have core or any other out-of-plane components for the case of zero current. However, under the

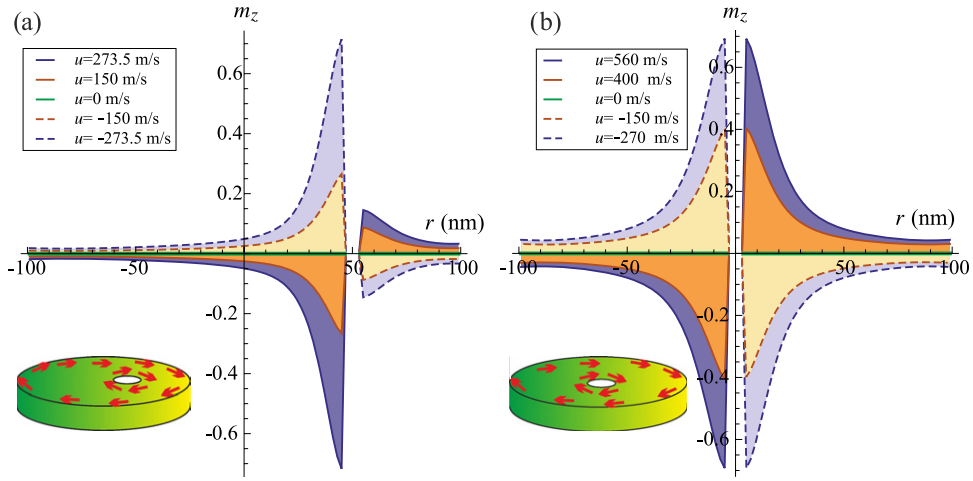

Figure 3. In-plane vortex profiles for different current values and vortex positions. Dashed and solid lines correspond to the opposite current directions. (*a*) shows profiles of the initially in-plane vortex pinned by the hole displaced by the value $L/2$ from the disc centre. (*b*) shows the similar profiles for the centred vortex. Simulations were performed for the permalloy disc with $L = 100$ nm and $h = 10$ nm for the case $\beta = 0$.

influence of the current there appears a dip-like out-of-plane structure. This dip structure has the following main properties. (i) The dip structure of the centred vortex is symmetrical and its sign is changed when the sign of u is changed, see figure 3(*b*). (ii) The skewness appears when the vortex is shifted and its value rapidly increases when the displacement s increases. (iii) The sign of the dip structure of the shifted vortex is determined by the sign of the product su and it has no direct relation to the vortex polarity. (iv) The critical current u_c takes maximal values for the centred vortex and decreases as the vortex displacement s increases. The detailed analytical description of the dip development, based on the magnon mode analysis, is under consideration; (v) dependence of $m_d(u)$ for the pinned vortex is well approximated by the expresstion

$$m_d \propto \sqrt{1 - \frac{u}{u_c}} - 1 \qquad (7)$$

in the whole range of values of u.

When the effective current velocity u achieves its critical value u_c, the vortex-antivortex pair is born on the edge of the inner hole. The antivortex falls into the hole (it annihilates with the pinned vortex), so finally the new vortex appears out of the hole. Polarity of the new born vortex p is equal to the polarity of the dip, in other words $p = -\text{sign}(us)$. In the case of centred vortex ($s = 0$) the polarity p is determined in a random way.

It is interesting to note that the critical current value depends on disc thickness and this dependence is different for free (out-of-plane) and pinned (planar) vortices, see figure 4. In the case of free vortex the critical velocity u_c weakly depends on thickness while in the case of pinned vortex this dependence is significant.

Taking into account the nonadiabatic term results the insignificant decrease in the critical current: for $\beta = 0.1$ the relative critical current shift $\Delta j_c/j_c \sim 10^{-3}$ and the corresponding dependences $m_d(u)$ are practically the same.

3. Discussion

Typically, to observe the vortex switching, one has to excite the low-frequency gyroscopical vortex motion. Therefore, it is difficult to distinguish the vortex motion and the dip creation process. That is why there exists a general opinion about dynamical origin of the vortex switching [40]; moreover, there is 'universal criterion' for the vortex switching, according to which the critical velocity of the vortex $u_c \sim 330\,\text{m}\,\text{s}^{-1}$ is required for the vortex core switching [35]. Recently we predicted the switching for the immobile vortex by a high-frequency rotating magnetic field [37]: the physical picture of the dip creation is softening of a high frequency azimuthal magnon mode due to the rotating field. However the mechanism of the dip creation in a low-frequency regime is still opened. In this paper we describes a set-up, which has all necessary features to study the dip creation process: it separates the dip creation processes from the vortex motion and provides the final state with a static vortex, shifted from the origin of the system.

It is instructive to discuss a relationship between the mechanisms of the dip creation for a moving vortex and a static vortex, shifted by a current. If the system allows the rigid motion with $\boldsymbol{m}(\boldsymbol{r}, t) = \boldsymbol{m}(\boldsymbol{r} - \boldsymbol{X}(t))$, the gyroscopic term $\mathscr{G} = -\frac{M_S}{\gamma}(1 - m_z)(\dot{\boldsymbol{X}} \cdot \boldsymbol{\nabla}\phi)$ has the same structure as a spin-torque energy term $\mathscr{E}_{ST}$. Therefore, one can talk about a formal analogy between the vortex velocity $\dot{\boldsymbol{X}}$ and the effective current velocity $\boldsymbol{u}$. The main difference is that the vortex motion is possible due to the gyroscopical properties of the out-of-plane vortex, and the pure planar vortex does not move at all, while the spin-current interaction is caused by the in-plane vortex structure, so it is almost the same for the out-of-plane vortex in disc and the planar vortex in rings. The origin of the dip creation is, in both cases, the excitations of magnon modes in the presence of magnetization inhomogeneity caused by the in-plane vortex structure.

In conclusion, we found that immobile planar vortex in a nanoring forms a dip structure under the action of adiabatic

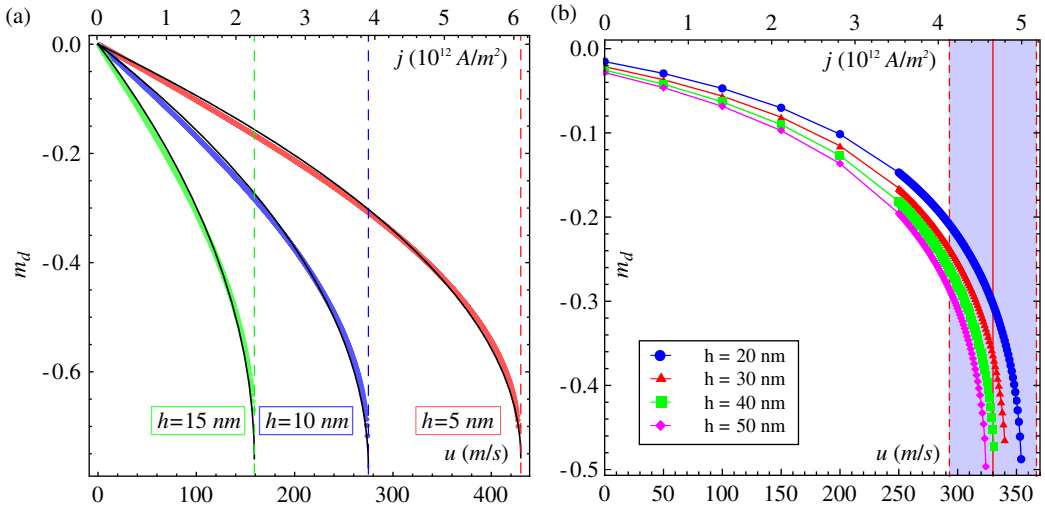

Figure 4. Dependences of the dip depth on the applied current for different thicknesses. (*a*) In-plane vortex is pinned on the hole with $s = 0.5$, (*b*) free out-of-plane vortex. Solid black lines demonstrate the dependence (7). The critical velocity $u_c = 330 \pm 37$ m s^{-1} which was determined in [35] is shown in the (*b*) as a vertical strip. The simulations are performed for samples with radius $L = 100$ nm for case $\beta = 0$.

spin current under the threshold value. Above its value the vortex–antivortex pair can be nucleated, which can cause the vortex switching process.

Acknowledgments

The authors acknowledge the support from Deutsches Zentrum für Luft- und Raumfart e.V., Internationales Büro des BMBF in the frame of a bilateral scientific cooperation between Ukraine and Germany, project No UKR 08/001. DDS thanks the University of Bayreuth, where a part of this work was performed, for kind hospitality and acknowledges the support from the Alexander von Humboldt Foundation.

References

[1] Zutic I, Fabian J and Sarma S D 2004 *Rev. Mod. Phys.* **76** 323
[2] Tserkovnyak Y, Brataas A, Bauer G E W and Halperin B I 2005 *Rev. Mod. Phys.* **77** 1375
[3] Pribiag V S, Krivorotov I N, Fuchs G D, Braganca P M, Ozatay O, Sankey J C, Ralph D C and Buhrman R A 2007 *Nature Phys.* **3** 498
[4] Mistral Q, van Kampen M, Hrkac G, Kim J-V, Devolder T, Crozat P, Chappert C, Lagae L and Schrefl T 2008 *Phys. Rev. Lett.* **100** 257201
[5] Ivanov B A and Zaspel C E 2007 *Phys. Rev. Lett.* **99** 247208
[6] Sheka D D, Gaididei Y and Mertens F G 2008 *Electromagnetic, Magnetostatic, and Exchange-Interaction Vortices in Confined Magnetic Structures* ed E Kamenetskii (Kerala: Research Signpost) pp 59–75
[7] Khvalkovskiy A V, Grollier J, Dussaux A, Zvezdin K A and Cros V 2009 *Phys. Rev.* B **80** 140401
[8] Gaididei Y, Kravchuk V P and Sheka D D 2010 *Int. J. Quantum Chem.* **110** 83
[9] Dussaux A *et al* 2010 *Nature Commun.* **1** 1
[10] Locatelli N, Naletov V V, Grollier J, de Loubens G, Cros V, Deranlot C, Ulysse C, Faini G, Klein O and Fert A 2011 *Appl. Phys. Lett.* **98** 062501
[11] Zhang S and Li Z 2004 *Phys. Rev. Lett.* **93** 127204
[12] Thiaville A, Nakatani Y, Miltat J and Suzuki Y 2005 *Europhys. Lett.* **69** 990
[13] Shibata J, Nakatani Y, Tatara G, Kohno H and Otani Y 2006 *Phys. Rev.* B **73** 020403
[14] Caputo J-G, Gaididei Y, Mertens F G and Sheka D D 2007 *Phys. Rev. Lett.* **98** 056604
[15] Sheka D D, Gaididei Y and Mertens F G 2007 *Appl. Phys. Lett.* **91** 082509
[16] Yamada K, Kasai S, Nakatani Y, Kobayashi K, Kohno H, Thiaville A and Ono T 2007 *Nature Mater* **6** 270
[17] Bolte M *et al* 2008 *Phys. Rev. Lett.* **100** 176601
[18] Choi Y-S, Yoo M-W, Lee K-S, Yu Y-S, Jung H and Kim S-K 2010 *Appl. Phys. Lett.* **96** 072507
[19] Cowburn R P 2007 *Nature Mater* **6** 255
[20] Tang D D and Lee Y-J 2010 *Magnetic Memory—Fundamentals and Technology* (Cambridge: Cambridge University Press)
[21] Van Waeyenberge B *et al* 2006 *Nature* **444** 461
[22] Xiao Q F, Rudge J, Choi B C, Hong Y K and Donohoe G 2006 *Appl. Phys. Lett.* **89** 262507
[23] Hertel R, Gliga S, Fähnle M and Schneider C M 2007 *Phys. Rev. Lett.* **98** 117201
[24] Lee K-S, Guslienko K Y, Lee J-Y and Kim S-K 2007 *Phys. Rev.* B **76** 174410
[25] Kravchuk V P, Sheka D D, Gaididei Y and Mertens F G 2007 *J. Appl. Phys.* **102** 043908
[26] Liu Y, He H and Zhang Z 2007 *Appl. Phys. Lett.* **91** 242501
[27] Vansteenkiste A *et al* 2009 *Nature Phys.* **5** 332
[28] Weigand M *et al* 2009 *Phys. Rev. Lett.* **102** 077201
[29] Novosad V, Fradin F Y, Roy P E, Buchanan K S, Guslienko K Y and Bader S D 2005 *Phys. Rev.* B **72** 024455
[30] Gaididei Y B, Kravchuk V P, Sheka D D and Mertens F G 2008 *Low Temp. Phys.* **34** 528
[31] Komineas S and Papanicolaou N 2010 *J. Math. Phys.* **51** 042705
[32] Gioia G and James R D 1997 *Proc. R. Soc. Lond.* A **453** 213
[33] Thiele A A 1973 *Phys. Rev. Lett.* **30** 230
[34] Thiele A A 1974 *J. Appl. Phys.* **45** 377
[35] Lee K-S, Kim S-K, Yu Y-S, Choi Y-S, Guslienko K Y, Jung H and Fischer P 2008 *Phys. Rev. Lett.* **101** 267206

[36] Mertens F G, Wysin G M, Völkel A R, Bishop A R and Schnitzer H J 1994 *Nonlinear Coherent Strutcures in Physics and Biology* ed F G Mertens and K H Spatschek (New York: Plenum) pp 191–7
[37] Kravchuk V P, Gaididei Y and Sheka D D 2009 *Phys. Rev.* B **80** 100405
[38] Gaididei Y, Kravchuk V P, Sheka D D and Mertens F G 2010 *Phys. Rev.* B **81** 094431
[39] Kravchuk V P, Sheka D D and Gaididei Y B 2007 *J. Magn. Magn. Mater.* **310** 116
[40] Guslienko K Y, Lee K-S and Kim S-K 2008 *Phys. Rev. Lett.* **100** 027203